Prediction of Pressure Drop in Straight Vortex Tubes

WILLIAM J. LOVE*
University of Washington, Seattle, Wash.

A simple flow model was developed for the purpose of estimating the pressure drop along a tube supplied with swirling flow. The model indicates that the energy losses observed for swirling flow can be orders of magnitude greater than that computed for comparable nonswirling flow. The losses are explained as due not only to the decay of the swirl, but also as a function of the axial flow area restriction caused by the swirl induced recirculating core. The results of analysis with the proposed model compared favorably with experimental data.

Nomenclature

E	= energy
f	= friction factor
f_R	= Blasius friction factor computed for the nonswirl condition of Reynolds number $2r_0W_{ave}/\nu$
f_θ	= friction factor, from Kinney[8]
F	= a pressure loss multiplier containing the correction for vorticity
$J \equiv \frac{V_0}{W_{ave}} = \frac{\pi r_0^2 V_0}{Q}$	= local vorticity characteristic
p	= static pressure
$p_w \equiv \frac{\rho_0 W_{ave}^2}{2}$	= dynamic pressure head in the absence of swirl
Q	= volumetric flow in tube
r, θ, z	= radial, tangential, and axial coordinate
$Re \equiv 2Q/\pi r_0 \nu$	= Reynolds number
U, V, W	= radial, tangential, and axial velocity, respectively
Z	= an energy loss multiplier containing the correction for kinetic energy losses
γ	= weight density
ν	= kinematic viscosity
ρ	= mass density
ϕ	= flow angle
τ	= shear stress

Subscripts

ave	= average value across the section
c	= zone of reversed axial flow
e	= condition at entrance into the tube
i	= zone of transition from free to forced vortex flow
o	= tube wall location
r, θ, z	= radial, tangential, and axial coordinate
t	= total

I. Introduction

THE evaluation of performance and the design optimization of vortex tube devices such as a vortex valve discharge tube or an axial vortex separator requires that the pressure drop and energy loss be estimated as a function of the inlet swirl and length. An obvious energy loss sustained in swirling flow is that encountered by the decay of the vorticity in the swirling flow. Another loss attributable to swirl is less obvious since it is introduced by the reduction or reversal of the axial velocity in the core of the vortex. This effect increases the axial flow velocity within an outer annular zone of the tube and intensifies the energy dissipation attributable to the axial flow component.

A simple model for swirl induced recirculation has been constructed for the purpose of estimating the pressure drop along a tube wall. This model was initially conceived in the course of study of a transparent, water driven vortex valve and discharge tube. During operation it was observed that a distinct vapor-gas core formed in the discharge tube under conditions of significant vorticity. Under conditions of tangential entry into the valve spin chamber, the core included more than 80% of the tube diameter.

The static pressure in this core was above saturation and constant along discharge tube axis. The core diameter increased slowly with time following an increase in vortex strength, indicating that the core was formed of gases which had dissociated from the water. Once formed, the core was quite stable; its diameter changed only gradually with axial position. The small voids at the exit tail of the core would oscillate slowly on the tube axis. Occasionally a bubble would move a bit further downstream at which point it would then be rapidly swept out of the tube. The braided, helical appearance of the liquid-gas core indicated that the axial velocity component was relatively low at the interface.

The pressure drop measured at the tube wall between the inlet and exit of the discharge tube was almost two orders of magnitude larger than that predicted for nonswirl flow. This wall pressure drop was essentially independent of the existence of a visible gas core, indicating that the tube flow characteristic had not been changed significantly by the properties of the core fluid.

The abovementioned observations suggested a flow model in which the fluid core recirculated and is stationary, and the shear stress at the core boundary is small relative to the other stresses acting upon the fluid between the core and the tube wall. The pressure loss prediction of an early version of this model was evaluated by Wallis[1] for small swirl values and found to be in reasonable agreement with the literature.[2,3] As will be shown, it also agrees favorably with the data of Youssef[4] covering swirling flow over a relatively wide range of flow conditions.

II. Analysis

The aforementioned flow observations provide the basis for an inviscid flow model in which the dissipative effects of turbulence are introduced as wall shear stresses. The equations of motion for steady, axisymmetric flow may be derived from the Navier-Stokes equations in cylindrical coordinates.[5]

The equation of continuity is

$$\frac{1}{r}\frac{\partial(rU)}{\partial r} + \frac{\partial W}{\partial z} = 0 \tag{1}$$

The momentum equations are

$$\rho\left(\frac{U\,\partial U}{\partial r} + \frac{W\,\partial U}{\partial z} - \frac{V^2}{r}\right) = \frac{-\partial p}{\partial r} + \frac{\partial \tau_{rz}}{\partial z} \tag{2}$$

Received August 1, 1973; revision received January 28, 1974. A major portion of the reported work was done during the author's employment by the General Electric Co., Schenectady, N.Y. The author gratefully acknowledges the comments and critical review of N. Lipstein during the progress of the work.

Index category: Nozzle and Channel Flow.

* Professor, Mechanical Engineering Department.

$$\rho\left(\frac{U}{r}\frac{\partial Vr}{\partial r}+\frac{W\partial V}{\partial z}\right)=\frac{1}{r^2}\frac{\partial(\tau_{\theta r}r^2)}{\partial r}+\frac{\partial\tau_{\theta z}}{\partial z} \tag{3}$$

$$\rho\left(\frac{U\partial W}{\partial r}+\frac{W\partial W}{\partial z}\right)=\frac{-\partial p}{\partial z}+\frac{1}{r}\frac{\partial(\tau_{zr}r)}{\partial r} \tag{4}$$

The following assumptions were used for the simplification and solution of the foregoing equations and pertain to the annular irrotational region of flow in a confining tube of radius r_0.

1) The vortex flow at any axial position is essentially irrotational with the exception of the close vicinity of the tube wall. The tangential velocity profile is thereby characterized by $V \simeq V_0(z)(r_0/r)$.

2) The radial pressure gradient at any axial position is positive because of the vortex flow. Therefore, the static pressure in the interior of the tube will be lower than that at the wall. Thus, although the axial pressure gradient at the tube wall is negative, there is a radial position, $r_i(z)$, at which the static pressure gradient is zero valued, $(\partial p/\partial z)_{r_i} \simeq 0$. At smaller radii, $r < r_i$, the positive radial pressure gradient can exceed the negative axial gradient at the wall and the resulting positive value of axial pressure gradient in the core location will act to decelerate and reverse the axial flow.

The shear stresses at the core interface are small and may be neglected relative to the tube wall stress, $(\tau_{r\theta})_{r_i} = 0$, $(\tau_{rz})_{r_i} = 0$. The net axial flow across the core section defined by r_i is zero valued, e.g.,

$$Q = 2\pi\int_{r_i}^{r_0} Wr\,dr$$

As mentioned earlier, this definition of the limit of the recirculating core was suggested by the data of Youssef[4] and Thompson.[6] It received further confirmation from the incompressible vortex valve discharge tube tests described in the Introduction.

3) Flow variations in the radial direction are small compared with corresponding variations in the axial direction. In accordance with the introductory observations, the radial velocity component is considered to be negligibly small compared with other components. Therefore, $U \simeq 0$, $\partial\tau_{rz}/\partial z \simeq 0$, and $\partial\tau_{\theta z}/\partial\theta \simeq 0$.

4) The wall shear stresses may be replaced by components in the form of a Blasius friction formula or its equivalent as modified for the presence of secondary flows such as Taylor Görtler vortices

$$\tau_{r_0} \equiv (-f/8)\rho[\bar{U}^2+\bar{V}^2+\bar{W}^2]$$

where the bar signifies a mean or characteristic velocity in the tube. Due to the uncertainty concerning the mean values to be used, this method is discussed in the Appendix in greater detail. The components of shear stress are defined by

$$(\tau_{rz})_{r_0} \equiv \tau_{r_0}\frac{\bar{W}}{(\bar{U}^2+\bar{V}^2+\bar{W}^2)^{1/2}}$$
$$(\tau_{r\theta})_{r_0} \equiv \tau_{r_0}\frac{\bar{V}}{(\bar{U}^2+\bar{V}^2+\bar{W}^2)^{1/2}} \tag{5}$$

The radial momentum equation (2) was modified and integrated using assumptions (1) and (3)

$$\rho(r_0^2V_0^2/r^3) = \partial p/\partial r \tag{6}$$

$$\int_r^{r_0}\frac{\partial p}{\partial r}dr = p(r_0,z)-p(r,z) = \frac{\rho V_0^2}{2}\left[\left(\frac{r_0}{r}\right)^2-1\right] \tag{7}$$

The axial gradient of the static pressure at the tube wall is

$$\frac{\partial p(r_0,z)}{\partial z} = \frac{dp(r_0z)}{dz} = \frac{\partial p}{\partial z}+\rho V_0\frac{\partial V_0}{\partial z}\left[\left(\frac{r_0}{r}\right)^2-1\right] \tag{8}$$

The core interface condition of assumption (3) is reduced to

$$dp(r_0,z)/dz = \rho V_0(\partial V_0/\partial z)[(r_0/r_i)^2-1] \tag{9}$$

The tangential momentum equation (1) was modified and integrated using the assumptions (1–3)

$$\rho r_0\frac{\partial V_0}{\partial z}\int_r^{r_0} Wr\,dr \simeq \int_r^{r_0}\frac{\partial(r^2\tau_{r\theta})}{\partial r}dr, \qquad r_i \leqq r \leqq r_0 \tag{10}$$

Assumption (3) provides a further simplification

$$\rho(Q/2\pi)\,dV_0/dz \simeq r_0\tau_{r_0\theta} \tag{11}$$

where

$$\int_{r_i}^{r_0} Wr\,dr \simeq \int_0^{r_0} Wr\,dr = \frac{Q}{2\pi} \tag{12}$$

The axial momentum equation (4) was simplified with assumption (3)

$$\rho W\frac{\partial W}{\partial z} = -\frac{\partial p}{\partial z}+\frac{1}{r}\frac{\partial(r\tau_{rz})}{\partial z} \tag{13}$$

The axial and tangential momentum equations (8) and (13) may be combined and integrated over the outer flow annulus to give

$$\frac{\partial p(r_0,z)}{\partial z}\int_{r_i}^{r_0} r\,dr+\rho\frac{\partial}{\partial z}\int_{r_i}^{r_0}\frac{W^2}{2}r\,dr = \int_{r_i}^{r_0}\frac{\partial(r\tau_{rz})}{\partial r}dr+\rho V_0\frac{\partial V_0}{\partial z}\int_{r_i}^{r_0}\left[\left(\frac{r_0}{r}\right)^2-1\right]r\,dr \tag{14}$$

The axial momentum integral may be replaced with an averaged term and a momentum correction factor, β, to account for the variation of axial velocity across the section

$$\int_{r_i}^{r_0} W^2r\,dr \equiv \beta\frac{Q^2}{2\pi^2r_0^2}\frac{1}{[1-(r_i/r_0)^2]} \tag{15}$$

Upon the inclusion of assumptions (3) and (4) and Eqs. (9) and (11), Eq. (14) may be converted to

$$\left(\frac{\pi r_0^2V_0}{Q}\right)\left[\left(\frac{r_i}{r_0}\right)^2-1-\ln\left(\frac{r_i}{r_0}\right)^2\right]+\frac{\beta}{2}\frac{\partial\left(\frac{1}{[1-(r_i/r_0)^2]}\right)}{\partial(\pi r_0^2V_0/Q)} \simeq \frac{\bar{W}}{\bar{V}} \tag{16}$$

since $(\tau_{r\theta}/\tau_{rz})_{r_0} = \bar{V}/\bar{W}\tan\phi_0$ as defined in the Appendix. Using method (1) of the Appendix to describe the tube wall shear stress, $\tan\phi_0 = J[1-(r_i/r_0)^2]$ and thus Eq. (16) becomes

$$J^2\left[1-\left(\frac{r_i}{r_0}\right)^2\right]\left[\left(\frac{r_i}{r_0}\right)^2-1-\ln\left(\frac{r_0}{r_i}\right)^2\right]-\frac{\beta}{2}\frac{J}{[1-(r_i/r_0)^2]}\frac{d[1-(r_i/r_0)^2]}{dJ} \simeq 1 \tag{17}$$

The numerical solution of this equation is shown in Fig. 1 along with those resulting from the use of methods (2) and (3) of the Appendix. The value $\beta = 1$ was used throughout since the

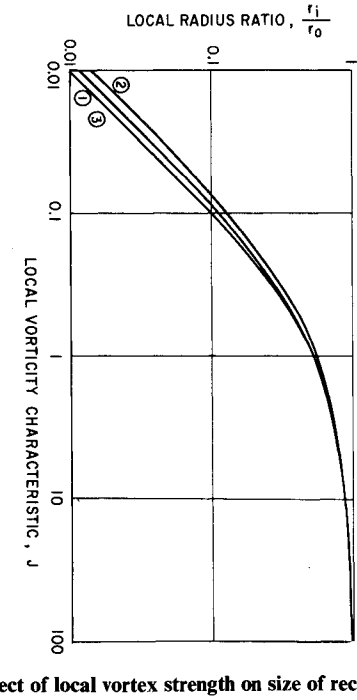

Fig. 1 Effect of local vortex strength on size of recirculating core.

numerical results showed only minor sensitivity to the value used.

Method (1) will be used in the remainder of this section to demonstrate the analytical approach. Equation (16) thus establishes a relation between the local core size r_i/r_0 and the local ratio of the circulation/axial flow, a local vorticity characteristic, $J \equiv (\pi r_0^2 V_0/Q)$.

Decay of Circulation

The decay of the circulation in the annular flow region surrounding the core may now be derived from Eq. (11) and the conditions of assumption (4)

$$\rho \frac{Q dV_0}{2\pi dz} = -r_0 \frac{f}{8} \rho [\bar{V}^2 + \bar{W}^2]^{1/2} \bar{V}$$

or

$$\frac{1}{J^2}\frac{dJ}{dz} = \frac{-f}{4r_0}\left[1 + \left(\frac{\bar{W}}{\bar{V}}\right)^2\right]^{1/2}\left(\frac{\bar{V}}{V_0}\right)^2 \tag{18}$$

This equation was solved using the methods described in the Appendix and the results are shown in Fig. 2. For example, using method (1) of the Appendix, Eq. (18) becomes

$$\frac{1}{J^2}\frac{dJ}{dz} = \frac{-f}{4r_0}\left(1 + \frac{1}{J^2[1-(r_i/r_0)^2]^2}\right) \tag{19}$$

which is solvable since the relationship between J and r_i/r_0 has been established by the solution of Eq. (17).

Local Static Pressure Drop

The static pressure drop at the tube wall may be found with Eq. (9)

$$\frac{dp(r_0, z)}{dz} = \rho V_0 \frac{dV_0}{dz}\left[\left(\frac{r_0}{r_i}\right)^2 - 1\right] \equiv -\frac{f_R}{4r_0}\rho\left(\frac{Q}{\pi r_0^2}\right)^2 F \tag{20}$$

where the Blasius friction factor for axial flow, f_R, is a function of the averaged axial Reynolds number, $Re \equiv 2Q/\pi r_0 \nu$. A local pressure loss multiplier, F, may now be introduced which will allow the correction of the tube pressure drop, as computed for the condition of nonswirl, to that with swirl. Therefore, upon substitution of Eq. (18)

$$F = \frac{4r_0}{f_R} J \frac{dJ}{dz}\left[\left(\frac{r_0}{r_i}\right)^2 - 1\right] = \frac{f}{f_R} J^3 \left[1 + \left(\frac{\bar{W}}{\bar{V}}\right)^2\right]^{1/2}\left(\frac{\bar{V}}{V_0}\right)^2\left[\left(\frac{r_0}{r_i}\right)^2 - 1\right] \tag{21}$$

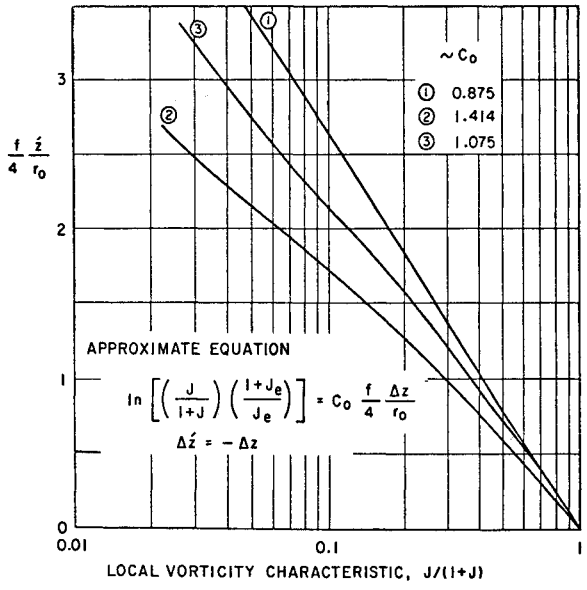

Fig. 2 Decay of vortex strength in a tube.

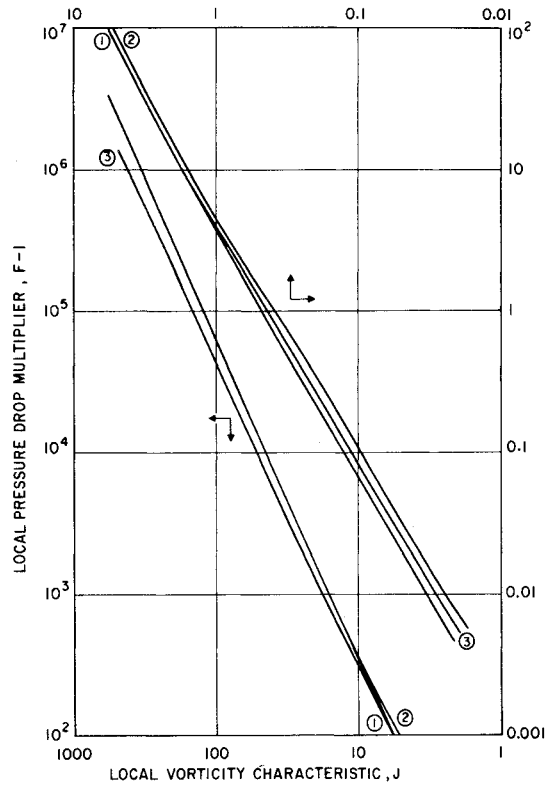

Fig. 3 Effect of local vortex strength upon local, axial pressure drop.

Using method (1) of the Appendix and approximating†

$$f/f_R \simeq 1$$

$$F \simeq J^3\left(1 + \frac{1}{J^2[1-(r_i/r_0)^2]}\right)\left[\left(\frac{r_0}{r_i}\right)^2 - 1\right] \tag{22}$$

The numerical results for the boundary methods described in the Appendix are shown in Fig. 3 where the value $F-1$ has been plotted in a manner to demonstrate the character of this function at low swirl values.

Average Static Pressure Drop

The static pressure drop at the tube wall from the tube inlet to the tube exit may be developed using the integrated value of the local pressure loss multiplier

$$\Delta p(r_0) = \int_{z_{\text{inlet}}}^{z_{\text{exit}}} \frac{dp(r_0, z)}{dz} dz \tag{23}$$

$$\Delta p(r_0) \equiv (-f_R/4r_0)(Q/\pi r_0^2)^2 F_{\text{ave}} \tag{24}$$

Therefore

$$F_{\text{ave}} \equiv \frac{1}{\Delta z}\int_{z_{\text{inlet}}}^{z_{\text{exit}}} F\, dz \tag{25}$$

For numerical analysis, it was found desirable to restate this expression as

$$(F_{\text{ave}} - 1) = \frac{1}{\Delta z}\int_{z_{\text{inlet}}}^{z_{\text{exit}}} (F-1)\, dz \tag{26}$$

Combining this expression with Eq. (18) results in

$$(F_{\text{ave}} - 1)\frac{f\Delta z}{2r_0} = 2\int_{J_{\text{inlet}}}^{J_{\text{exit}}} \frac{(F-1)\, dJ}{J^2[1+(\bar{W}/\bar{V})^2]^{1/2}(\bar{V}/V_0)^2} \equiv 2[I(J_{\text{inlet}}) - I(J_{\text{exit}})] \tag{27}$$

This expression was integrated numerically for the wall conditions described in the Appendix and the results are shown in Fig. 4.

† At this point such an approximation is made strictly for convenience. Its applicability will be discussed further.

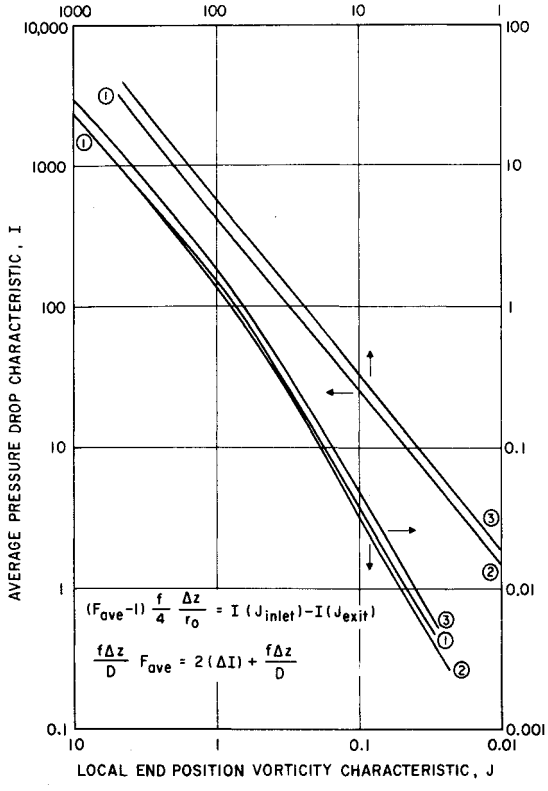

Fig. 4 Effect of over-all vortex strength change and tube length upon average axial pressure drop.

Total Energy Loss

The flow conditions for the outer annular flow have been described earlier and are extended here to include the core region. For simplicity, the core velocity profiles are considered as linear relationships. These profiles assume that the flow in the outer annulus is that of a free vortex whereas the recirculation flow in the core is that of a forced vortex. The total flow in the outer annulus is assumed equal to the total tube flow and the net flow in the core is zero valued

$$\begin{aligned} r > r_i, \quad & V_r = V_0 r_0, \quad W = W_0 \\ r < r_i, \quad & \frac{V}{r} = \frac{V_0 r_0}{r_i^2}, \quad W = \left(3\frac{r}{r_i} - 2\right) W_0 \\ & Q = W_0 \pi (r_0^2 - r_i^2) \end{aligned} \tag{28}$$

The axial flow profile in the core follows that reported by Youssef[4] and Wallis[1] when approximated by straight line functions.

The total flow energy is composed of the static and velocity heads. The energy terms are

$$E_{press} = 2\pi \int_0^{r_0} pWr\,dr \quad \text{where} \quad p_0 - p = \int_r^{r_0} \rho \frac{V}{r}\,dr \tag{29}$$

$$E_{axial} = 2\pi \int_0^{r_0} \frac{\rho W^2}{2} Wr\,dr \tag{30}$$

$$E_{tang} = 2\pi \int_0^{r_0} \frac{\rho V^2}{2} Wr\,dr \tag{31}$$

The energy per unit volume of flow under the assumed velocity profiles may be computed from the foregoing equations as

$$\frac{E_{total}}{Q} = \frac{E_{press}}{Q} + \frac{E_{tang}}{Q} + \frac{E_{axial}}{Q} = p_0 + \frac{p_w}{1-(r_i/r_0)^2} \times \left\{\left[1.4 - \left(\frac{r_i}{r_0}\right)^2\right] J^2 + \frac{1}{1-(r_i/r_0)^2}\left[1 - \frac{0.2}{(r_0/r_i)^2 - 1}\right]\right\}$$

where

$$p_w \equiv \rho W_{ave}^2/2 \tag{32}$$

The pressure drop along the tube wall and the core radius ratio have been derived as functions of a characteristic flow angle [see Eq. (24)]. In the same manner, the total energy loss per unit volume

$$\frac{E_{tot}/Q}{p_w} = \left(\frac{f\Delta z}{2r_0}\right) F_{ave}\Big|_2^1 + \Delta Z\Big|_2^1 \tag{33}$$

where

$$Z \equiv \frac{1}{1-(r_i/r_0)^2}\left\{\left[1.4 - \left(\frac{r_i}{r_0}\right)^2\right] J^2 + \left[1 - \frac{0.2}{(r_0/r_i)^2 - 1}\right]\frac{1}{1-(r_i/r_0)^2}\right\} \tag{34}$$

The characteristic Z is shown in Fig. 5 as derived from method (1) of the Appendix.

Comparison with Experimental Data

The foregoing derivations were compared with the experimental results of Youssef.[4] This was the most complete experimental data available for comparison purposes. Youssef conducted a series of air tests in a $12\frac{1}{4}$ in. i.d., 32-ft long tube, atmospheric exit, in which the entrance swirl could be controlled by adjustable stationary blades. Velocity flow angle, and static pressure measurements were made at various stations using an all-attitude, five-hole pressure probe. Data was reported for three swirl blade, weight-flow settings and at five axial locations, 2.5, 7.5, 10, 20, and 30 ft.

The pertinent data was abstracted from the report, reduced and compared directly with the analytical predictions which resulted from the use of the characteristics shown in Figs. 1–5.‡ The input value of swirl used in the analytical predictions is the local vorticity characteristic taken from the experimental data. The appropriate experimental and computed values are compared in Figs. 6–9. The 2.5-ft axial location data has been delineated since the effect of the inlet swirl blades is still very much in evidence at that position.

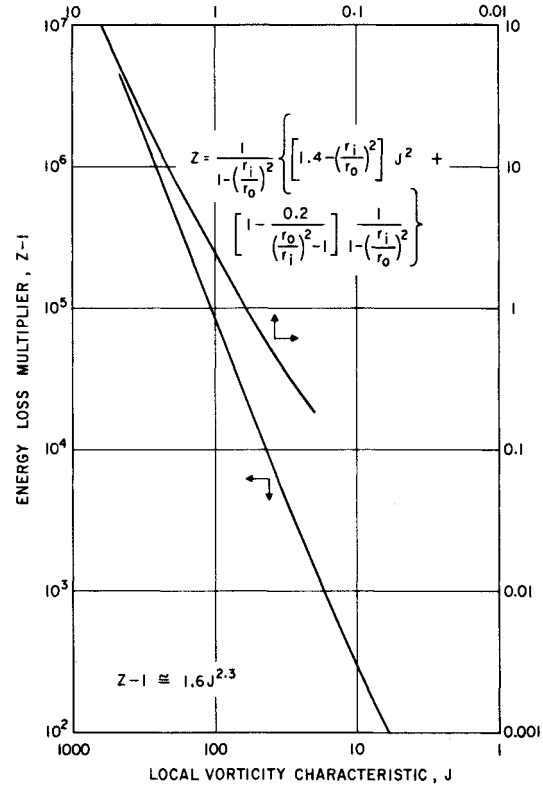

Fig. 5 Energy loss characteristic.

‡ Tables of the experimental and analytical results may be obtained by request from the author.

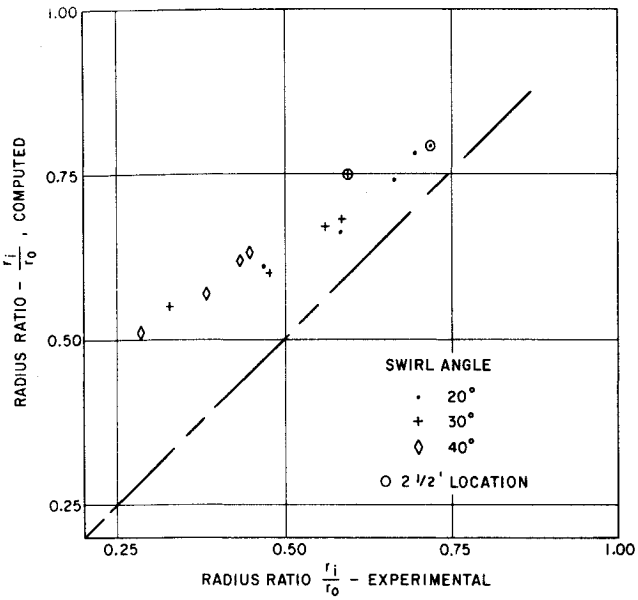

Fig. 6 Comparison of experimental vs computed radius ratio.

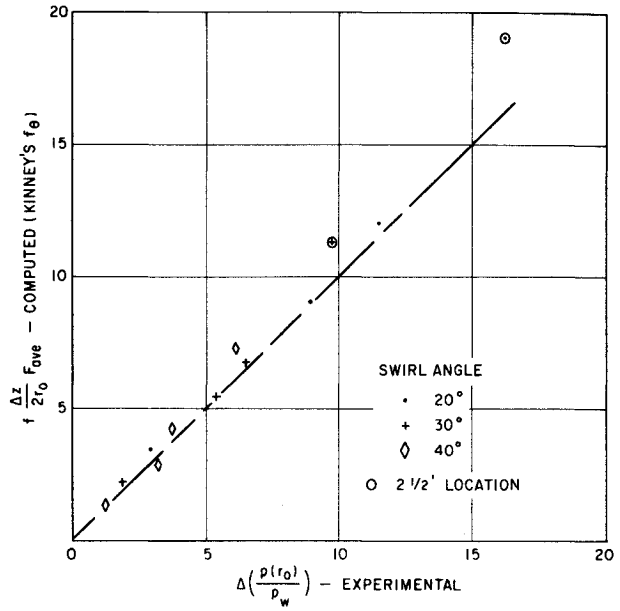

Fig. 8 Comparison of Kinney vs computed vortex decay characteristic.

The radius ratio defining the zero net flow core, Fig. 6, is consistently overestimated by the analytical model, particularly at the smaller values of local vorticity.

The decay of local vorticity along the tube, Fig. 7, is consistently underestimated using the conventional Blasius assumption for wall friction. The error in effective friction factor, using method (3) of Fig. 2, is about $\frac{3}{2}$. The presence of Görtler vortices in the outer annulus is suspected: increased mixing at the wall would reduce the boundary-layer thickness and increase the losses. Yeh[7] has observed a similar intensive boundary-layer turbulence next to the concave wall of an annulus with swirling flow.

Kinney[8] has developed a hypothesis for rotating cylinder flow in which the eddy diffusivity is constant over the central region of irrotational flow. Whereas the mean angular momentum in the case of flow between cylinders is approximately one-half of the angular momentum of the rotating cylinder, the mean angular momentum in the present case of swirling tube flow may be approximated directly from the extrapolated value of wall tangential velocity. Thus for fully established turbulence Kinney's Eq. (47),[8] may be expressed as

$$f_\theta = 8(F_\theta/\rho V_0^2) = 8(2K_4^2) = 0.025$$

The condition of fully established turbulence should hold for all tangential wall velocities reported by Youssef, due to the high Taylor number. A comparison of this friction value with experimentally determined values has been made in Fig. 10 and is quite favorable.

The pressure drop multiplier, Fig. 8, was estimated surprisingly well using the analytical model. Data at the 2.5-ft position near the inlet swirl vanes do not appear to be characteristic of the flow, due to the influence of inlet blades. It will be noted that the value of average multiplier, F_{ave}, occasionally approaches that of the local multiplier at low values of local vorticity. The graphical technique for F_{ave} uses Figs. 2 and 4 for $f\Delta\acute{z}/4r_0$ and $f\Delta\acute{z}/2r_0 F_{ave}$.

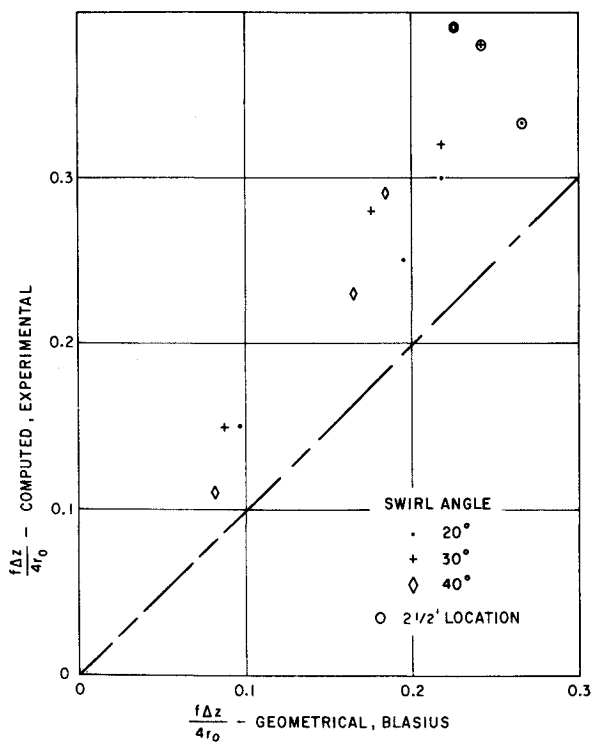

Fig. 7 Comparison of Blasius vs computed vortex decay.

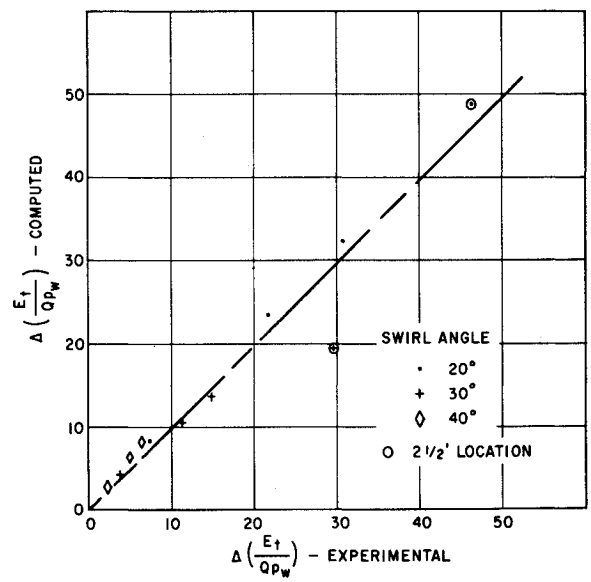

Fig. 9 Comparison of experimental vs computed axial wall pressure drop multiplier.

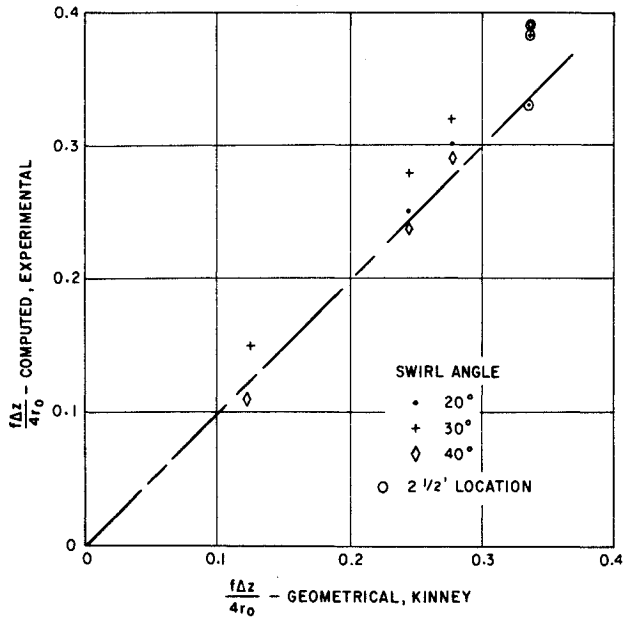

Fig. 10 Comparison of experimental vs computed average energy change.

Where small differences in local vorticity are involved, it may be advisable to utilize the local slope values of these curves to avoid the errors produced by the use of small differences between larger graphically determined values.

The average energy (or total pressure) change, Fig. 9, was estimated quite well with the analytical model. Again, the data near the inlet is suspect due to the influence of the inlet swirl vanes. This influence may be readily identified by inspection of Youssef's data as extending into the 7.5-ft axial location.

Baker's data[9] was analyzed in a similar manner for vortex decay and over-all pressure loss. While less extensive than Youssef's data, the results provided comparable agreement between experimental and predicted values.

Discussion

A significant difficulty in the estimate of the pressure drop loss to be expected in a long tube is the estimate of the decay of vortex strength as the flow passes down the tube. The visual examination of the core interface for water with an air purged core and the various concave wall flow stability criteria discussed by Schlichting[10] provide a strong indication of the presence of Taylor-Görtler vortices. Consequently, the wall shear stress may be expected to be significantly larger than that which would be predicted by conventional flat plate or nonswirling tube flow techniques. Other than Kinney's,[8] no work was found to directly define the wall shear stress in the presence of Görtler vortices.

The decay of vorticity in the tube appears to be approximated reasonably well by use of method (3) of the Appendix and the Taylor-Görtler friction factor of Kinney. While no evidence to the contrary has been evolved, it is rather obvious that the comparison of the model predictions with the test data should be considered fortuitous for the present and be verified with further experimental data when the opportunity permits.

The neglect of the radial flow in the analysis is not borne out by the test data of Youssef.[4] However, an unpublished reduction of that data shows that it will not satisfy the continuity equation without a significant reduction in radial velocity and its gradient. Thus, reasonable doubt exists as to the absolute magnitudes of Youssef's data for the radial velocity magnitude and gradient.

The lack of agreement between the computed vs experimental core radius is not surprising. The computed radius is based upon the assumption that the radius at which the axial static pressure gradient is zero valued is also that defining a zero valued net core flow. While it is obvious that a positive pressure gradient is required to produce a region of reversed flow, the assumption of the one being the delineator of the other is primarily an analytical convenience based only upon the introductory observation that this does indeed appear to occur when the core is purged with a gas.

In the foregoing, it has been suggested that the decay of vorticity has been increased by the presence of Taylor-Görtler vortices. The axial friction factor should also be correspondingly influenced by such an increase in boundary mixing. Yet, a good correlation of the pressure data was achieved using the conventional Blasius friction factor, e.g., $f/f_R \simeq 1$. The explanation may lie in the core radius prediction discussed previously. The analytical model consistently predicts a larger core than is observed and therefore should tend to predict a larger pressure drop than observed. As such the error in core geometry prediction would tend to offset the neglect of increased wall friction in the presence of Taylor-Görtler vortex circulation.

Appendix

Computation of a Nominal Shear Stress at the Wall of the Tube

The shear stresses at the wall were generated as components of a Blasius friction factor relationship following the approach of Schlichting.[11] Several possible shear stress velocity relationships were considered since there is no Blasius equivalent which includes the effect of flow over severe concave surfaces. Only the irrotational flow pattern of the outer annulus was considered.

Method (1)—Outer Wall Annular Flow Condition

$$\tau_{r_0} = \frac{-f}{8}\rho[V_0^2 + W_0^2] = \frac{-f}{8}\rho\left(J^2 + \frac{1}{[1-(r_i/r_0)^2]^2}\right)W_{\text{ave}}^2$$

$$W_{\text{ave}} \equiv \frac{Q}{\pi r_0^2}, \quad \tan\phi_0 \equiv \frac{V_0}{W_0} = J\left[1-\left(\frac{r_i}{r_0}\right)\right] = \frac{\tau_{r\theta}}{\tau_{zr}}$$

Method (2)—Average Outer Annular Flow Condition

$$\tau_{r_0} = (-f/8)\rho[V_{\text{ave}} + W_0]^2$$

where

$$V_{\text{ave}} = \frac{2}{r_0 - r_i}\int_{r_i}^{r_0} Vr\,dr = \frac{-f}{8}\rho\left[\left(\frac{2J}{1+(r_i/r_0)}\right)^2 + \frac{1}{[1-(r_i/r_0)^2]^2}\right]W_{\text{ave}}^2, \quad \tan\phi_0 = 2J\left[1-\left(\frac{r_i}{r_0}\right)\right] = \frac{\tau_{r\theta}}{\tau_{zr}}$$

Method (3)—Adapted from the $\frac{1}{7}$th Power Law[12]

$$\tau_{r_0} = 0.0225\rho(W/W_{\text{ave}})^{7/4}[V_\delta^2 + W^2]^{7/8}(\bar{y}/y_m)^{1/4}$$

where

$$V_\delta = V_0 r_0/r_\delta, \qquad y_m = r_0 - r_i$$

$$\bar{y}/y_m = (W_{\text{ave}}/W)^n, \qquad n = 7$$

$$\frac{W_{\text{ave}}}{W} = \frac{2n[n+(r_i/r_0)(1+n)]}{[1+(r_i/r_0)](1+n)(1+2n)}$$

$$\frac{r_0}{r_\delta} = \frac{1}{1-(\bar{y}/y_m)[1-(r_i/r_0)]}$$

$$\tau_{r_0} = \frac{0.0225(2)^{1/4}\rho}{Re^{1/4}}\left(\frac{W}{W_{\text{ave}}}\right)^{7/4}$$

multiplied by

$$\left[J^2\left(\frac{r_0}{r_\delta}\right)^2 + \frac{1}{1-(r_i/r_0)^2}\right]^{3/8}\frac{W_{\text{ave}}^2}{[1-(r_i/r_0)]^{1/4}}$$

$$\tan\phi_0 = V_\delta/\bar{W} = J[1-(r_i/r_0)^2]r_0/r_\delta = \tau_{r\theta}/\tau_{zr}$$

References

[1] Wallis, G. B., "Pressure Drop and Swirl Attenuation for Vortex Flow in a Straight Pipe," Internal Rept. 66-C-445, Nov. 1966, General Electric, Schenectady, N.Y.

[2] Kreith, F. and Sonju, O. K., "The Decay of a Turbulent Swirl in a Pipe," *Journal of Fluid Mechanics*, Vol. 22, No. 2, 1965, pp.257–271.
[3] Menis, M., "Effect of Vortex Decay on Pipe Flow," Rept. 61, Nov. 1960, Gas Turbine Lab., MIT, Cambridge, Mass.
[4] Youssef, T. E. A., "Some Investigations on Rotating Flow with a Recirculation Core in Straight Pipes," Paper 66-WA-FE-36, Nov. 27, 1966, American Society of Mechanical Engineers, New York.
[5] Schlichting, H., *Boundary Layer Theory*, 4th ed., McGraw-Hill, New York, 1960, pp. 53–54.
[6] Thompson, J. R., Jr., "The Structure of Free and Confined Turbulent Vortices," Research Note 44, May 1963, Aero Physics Dept., Mississippi State University, State College, Miss.
[7] Yeh, H., "Boundary Layer Along Annular Walls in a Swirling Flow," and "Discussion," *Transactions of the ASME*, May 1958, pp. 767–776.
[8] Kinney, R. B., "Universal Velocity Similarity in Fully Turbulent Rotating Flows," ASME Paper 67-APM-23, June 1967, Applied Mechanic Conference, Pasadena, Calif.
[9] Baker, D. W., "Decay of Swirling, Turbulent Flow of Incompressible Fluids in Long Pipes," Ph.D. thesis, 1967, Univ. of Maryland, College Park, Md.
[10] Schlichting, H., *Boundary Layer Theory*, 4th ed., McGraw-Hill, New York, 1960, pp. 441–444.
[11] Schlichting, H., *Boundary Layer Theory*, 4th ed., McGraw-Hill, New York, 1960, p. 503.
[12] Schlichting, H., *Boundary Layer Theory*, 4th ed., McGraw-Hill, New York, 1960, pp. 502–508.

JULY 1974 AIAA JOURNAL VOL. 12, NO. 7

Calculation of the Flow on a Cone at High Angle of Attack

STEPHEN C. LUBARD*
R & D Associates, Santa Monica, Calif.
AND
WILLIAM S. HELLIWELL†
The Aerospace Corporation, El Segundo, Calif.

A method of predicting the flowfield on cones at high angles of attack for the supersonic laminar case is developed in this paper. An approximate system of equations obtained from the steady-state Navier-Stokes equations by assuming the viscous, streamwise derivative terms are small compared with the viscous normal and circumferential derivatives is used. These equations are valid in both the viscous and inviscid regions including the circumferential separation zone which develops on the leeward side at the higher angles of attack. A new implicit differencing technique with iteration is used to solve the resulting three-dimensional parabolic equations. This differencing scheme permits the solution to problems at the higher Reynolds numbers (10^6). Predictions are compared with experimental data for a 10° half-angle cone at 12° angle of attack at a freestream Mach number of 8 and a 5.6° half-angle cone at 8° angle of attack at a freestream Mach number of 14. Very good agreement with the data is obtained for both of these cases.

Nomenclature

Cp = specific heat at constant pressure divided by the freestream value
f = represents any of the quantities differenced
∇G^2 = $[(\partial\xi/\partial x)^2+1+(1/r\,\partial\xi/\partial\phi)^2]$
h = enthalpy divided by freestream value
j = index in the x direction
k = conductivity divided by freestream value
k = index in the η direction
L = reference length
l = index in the ϕ direction
M_∞ = freestream Mach number
M_x = local streamwise Mach number, $M_\infty u/(h)^{1/2}$
p = pressure divided by twice the freestream dynamic pressure
Pr = freestream Prandtl number
Q = heat transfer to the surface
r = metric for the ϕ coordinate; $x\sin\theta+y\cos\theta$
Re = freestream Reynolds number based on L
u = velocity in the x direction divided by freestream velocity
v = velocity in the y direction divided by freestream velocity
V_∞ = freestream velocity
w = velocity in the ϕ direction divided by freestream velocity
$\bar{x}$ = x divided by x_o
x_o = value of x where the desired angle of attack is reached
x = coordinate along the rays of the cone surface divided by L
Δx = grid spacing in the x direction
y = coordinate normal to the surface divided by L
Δy = grid spacing in the y direction
α = angle of attack
γ = ratio of specific heats
δ = increment to be added to the known iterate
η = transformed normal coordinate
$\Delta\eta$ = grid spacing in the η direction
θ = cone half angle
λ = bulk viscosity divided by freestream viscosity $(-\frac{2}{3})\mu$
μ = viscosity divided by freestream viscosity
ξ = bow shock standoff distance divided by L
ρ = density divided by freestream density
ϕ = circumferential coordinate
$\Delta\phi$ = grid spacing in the ϕ direction

Subscripts

∞ = values in the freestream
k, l = values at the given grid point, $k\to\eta$; $l\to\phi$
K = grid points at the bow shock

Presented as Paper 73-636 at the AIAA 6th Fluid and Plasma Dynamics Conference, Palm Springs, Calif., July 16–18, 1973; submitted September 5, 1973; revision received January 28, 1974. The authors would like to express their gratitude to T. Kubota of the California Institute of Technology and F. Fernandez of R & D Associates for suggesting the problem and providing many helpful suggestions during the course of the research.
Index categories: Viscous Nonboundary-Layer Flows; Supersonic and Hypersonic Flow.
* Research Scientist. Associate Member AIAA.
† Member of the Technical Staff.